



# Tragacanth-mediate synthesis of NiO nanosheets for cytotoxicity and photocatalytic degradation of organic dyes

Zahra Sabouri<sup>1,2</sup> · Alireza Akbari<sup>2</sup> · Hasan Ali Hosseini<sup>2</sup> · Mehrdad Khatami<sup>3</sup> · Majid Darroudi<sup>4,5</sup>

Received: 5 December 2019 / Accepted: 19 February 2020 / Published online: 6 March 2020  
© Springer-Verlag GmbH Germany, part of Springer Nature 2020

## Abstract

In this study, NiO nanosheets have been manufactured using a co-precipitation approach that involved the usage of nickel nitrate ( $\text{Ni}(\text{NO}_3)_2 \cdot 6\text{H}_2\text{O}$ ) as the raw material and tragacanth in the role of a stabilizing agent. NiO nanosheets have been fabricated through the reduction of nickel nitrate solution that had been obtained by the application of aqueous extract of tragacanth, which is capable of functioning as a reducing and stabilizing agent. In the following, the physical and chemical properties of tragacanth-stabilized NiO nanosheets have been identified via FESEM, EDS, XRD, UV–Vis, and FT-IR techniques. According to the XRD pattern, these particular nanosheets have contained a cubic structure and group space Fm3m, along with the average size of about 18 to 43 nm that had been in agreement with the FESEM measurements. In addition, we have evaluated the photocatalytic activity of tragacanth-stabilized NiO nanosheets on the degradations of methylene blue (MB) and methyl orange (MO) dyes. The performed photocatalytic assessment has displayed that the nanosheets can degrade 82% of MO within 210 min and 60% of MB in 300 min. The cytotoxicity of tragacanth-stabilized NiO nanosheets on human Glioblastoma cancer (U87MG) cell lines has been investigated via the MTT assay, while it has been detected in the obtained results that the inhibitory concentration ( $\text{IC}_{50}$ ) had been 125  $\mu\text{g}/\text{mL}$ .

**Keywords** NiO nanosheets · Co-precipitation · Tragacanth-stabilized · Photocatalytic degradation · Cytotoxicity

## Introduction

Throughout the last decade, nanostructured materials have attracted the attention of many considering their attractive and unique properties as well as their superior applications compared to their non-nano counterparts [1]. The importance of nanostructured materials relies on the fact that the

capability of nanoscale substances in displaying different physical and chemical properties is quite different than their bulk material [2]. Among the various nanomaterials, metallic oxides have attracted a lot of attention in terms of environmental and medical applications [3–5], which is due to their interesting optical, magnetic [6], electrical, and photocatalytic properties [7], as well as the general qualities such as mechanical resistance, thermal stability, and chemical features [8]. Next to having a long history, photocatalytic processes have been used for many years as one of the environmental solutions throughout the industrialized countries [9, 10]. In the meantime, new photocatalytic materials with various properties are introduced daily to the market and put into utilization. In this study, NiO nanosheets have been utilized as photocatalyst to remove the organic pigments from aqueous environments [11]. Due to their high surface-to-volume ratio, NiO photocatalysis with high photocatalytic properties stands as one of the key technologies that are used in controlling the environmental pollutions [12, 13]. This technology can be extensively used to control the pollution of water treatment systems, wastewater, and air while providing a healthy environment by eliminating the chemical

✉ Majid Darroudi  
darroudim@mums.ac.ir; majiddarroudi@gmail.com

<sup>1</sup> Nanotechnology Research Center, Pharmaceutical Technology Institute, Mashhad University of Medical Sciences, Mashhad, Iran

<sup>2</sup> Chemistry Department, Payame Noor University, 19395-4697 Tehran, Iran

<sup>3</sup> NanoBioEletrochemistry Research Center, Bam University of Medical Sciences, Bam, Iran

<sup>4</sup> Nuclear Medicine Research Center, Mashhad University of Medical Sciences, Mashhad, Iran

<sup>5</sup> Department of Medical Biotechnology and Nanotechnology, Faculty of Medicine, Mashhad University of Medical Sciences, Mashhad, Iran

contaminants [14]. As an effect of UV light irradiation on NiO nanosheets, the formation of an electron–hole pair has been observed throughout the photocatalytic process [15]. Throughout a reduction reaction, electrons react with  $O_2$  molecular and produce superoxide anion radicals ( $\cdot O_2^-$ ), while in the course of an oxidative reaction, the produced holes with  $H_2O$  molecules result in the production of  $\cdot OH$  radicals. Next to being very energetic and reactive, these radicals ( $\cdot OH$ ,  $\cdot O_2^-$ ) can also react with organic compounds and various pollutants and lead to their decomposition [16]. Due to the breakdown of organic compounds' bonds and their decomposition, their toxic and hazardous properties have disappeared, which had resulted in the manufacturing of products that are far less dangerous and non-toxic than raw materials. In this paper, natural materials such as tragacanth have been used to synthesize NiO nanosheets since they have proved to be less dangerous for human health. Tragacanth is a dried gum discharge that is procured from several plant species and is known to be biodegradable and non-toxic. This material stands as a good base for the synthesis of NiO nanosheets [17]. Tragacanth is considered as a complex mixture of branched heteropolysaccharides that can be hydrolyzed in aqueous medium to various organic substances such as fucose, arabinose, galactose, xylose, and galactronic acid. Hydrolysis materials can be easily involved in the process of nuclearization and the growth of nucleus in solution, as well as functioning in the roles of capping and stabilizing agents [18, 19]. Considering their advantages such as simplicity, ease of growth, availability, flexibility to temperature, and pH, the utilization of polymeric and natural materials as reducing agents has turned green synthesis into a reliable and efficient method [20]. The green synthesis of nanosheets is a sustainable way in the field of chemistry and biotechnology that can be considered as a solution for the global problems of pollution and toxicity [21–23]. In regards to the synthesis of nanosheets, there has been a great deal of reported research on biosynthesis that involves the usage of plant extracts [24], fruit extracts, enzymes, polymeric material, fungi, and bacteria. Moreover, various procedures are applied for the production of NiO nanosheets that include sol–gel [25], microwave [26], ultrasonic, and co-precipitation [27]. Although the synthesis of NiO nanosheets have been carried out many times throughout the last decade, yet the exact mechanism of synthesis is still being investigated. Furthermore, finding the suitable polymer material that would be capable of synthesizing nanosheets in different sizes and shapes with high yields is also a challenge. In this research, we have reported the synthesis of tragacanth-stabilized NiO nanosheets through a co-precipitation method for the first time, while the utilized raw materials for this synthesis have been quiet inexpensive and included nickel salt, ammonia, and tragacanth-stabilized. This method has been observed to be faster than other procedures and because

of its non-solvent use, it has been labeled as a green and environmentally friendly technique. In this research, we have examined the cytotoxicity effects of tragacanth-stabilized NiO nanosheets on human glioblastoma cancer (U87MG) cells lines. Glioblastoma is an invasive tumor that is related to the central nervous system and is a common name for a type of brain tumor, while U87 (Uppsala 87) is known to be a human primary glioblastoma cell line [28, 29]. As a famous p-type semiconductor material, tragacanth-stabilized NiO nanosheets have a great potential for being utilized in catalysis and photocatalyst. Hence, the goal of this research was to synthesize tragacanth-stabilized NiO nanosheets through a co-precipitation method, and in the following, we have exhibited their application in investigating the cytotoxicity effects of these nanosheets on human Glioblastoma cancer (U87MG) cells lines via the MTT method. Also, we have evaluated the photocatalytic activity of tragacanth-stabilized NiO nanosheets on degradation methylene blue (MB) and methyl orange (MO) dyes. The photocatalytic assessment has displayed that tragacanth-stabilized NiO nanosheets can degrade 82% of MO within 210 min and 60% of MB in 300 min.

## Experimental section

### Materials

To perform the experiments of this study, nickel (II) nitrate [ $Ni(NO_3)_2 \cdot 6H_2O$ ] salt has been purchased from Merck, China, and used as the precursor for the synthesis of NiO nanosheets, ammonium hydroxide ( $NH_4OH$ ) has been procured from Sigma-Aldrich and tragacanth that functioned as the stabilizing agent has been collected from North Khorasan Province. The tragacanth specimen has been powdered using a mill and dissolved in distilled water. Then, the suspension has been kept for one day to obtain a complete water uptake.

### Green synthesis of NiO nanosheets

To begin the preparation of NiO nanosheets, 7.26 g of ( $Ni(NO_3)_2 \cdot 6H_2O$ ) has been dissolved in 50 mL of water solvent and stirred for 30 min. Simultaneously, 1.0 g of tragacanth has been dissolved in 50 mL of distilled water and stirred at 60 °C for 90 min until a clear and colorless solution had been obtained. Then, we have slowly appended nickel nitrate solution to the mixture of tragacanth. In the following, ammonium hydroxide solution ( $NH_4OH$ , 2.0 M) has been added in a drop-wise manner to the previous solution until the pH had been observed to reach around 9. The  $NH_4OH$  has functioned in the role of a precipitating agent and caused the formation of green sediment. The obtained powder has

been filtered and washed several times via distilled water and after that, had been dried at 120 °C for 12 h and calcined for 2 h at the temperatures of 300, 400, 500, and 600 °C, which is included as the following Eq. 1. Figure 1 demonstrates a schematic plan of NiO nanosheets biosynthesis.



### Photocatalytic test of tragacanth-stabilized NiO nanosheets for MB degradation

The photocatalytic experiment of synthesized tragacanth-stabilized NiO nanosheets has been examined regarding the degradation of methylene blue (MB) and methyl orange (MO) dyes. For this matter, 74 mg of tragacanth-stabilized NiO nanosheets have been immersed in a 100 mL solution that contained 3 mg (pH 9) of MB, and as the solution was being stirred, it has been exposed to the irradiated UVA (11 W) light. To determine the amount of dye degradation, 2 mL of the solution has been removed every 30 min while taking the UV–Vis spectrum, which had been repeated for up to 300 min. In all of the cases, the volume of the solution has been kept constant.

## Results and discussion

### Characterization of tragacanth-stabilized NiO nanosheets

Different analyzes are used to identify and confirm the synthesis of tragacanth-stabilized NiO nanosheets. The powder has been measured by FT-IR spectra (FT-IR 8400-SHIMADZU made in Germany) to identify the existing bonds and functional groups throughout the range of 4000–400  $\text{cm}^{-1}$ . To prepare the sample for this analysis, the synthesized powder has been mixed with KBr in a ratio of 1:100 and then applied to the device in the form of a tablet while being positioned in the path of the beam for measurement. The XRD analysis (D8-Advance Bruker made in Germany) has been carried out through the usage of  $\text{Cu } K_\alpha$  radiation ( $k = 1.5418 \text{ \AA}$ ) in the Bragg range of  $80 > 2\theta > 10$ , which had been performed to determine the phases and detect the crystalline structure of nanosheets. The morphology of tragacanth-stabilized NiO nanosheets has been ascertained by FESEM and EDX analyzes (TESCAN BRNO-Mira3 LMU made in Germany). We have coupled the FESEM images with EDX analysis for morphological purposes and to determine the constituent elements and purity of biosynthesized

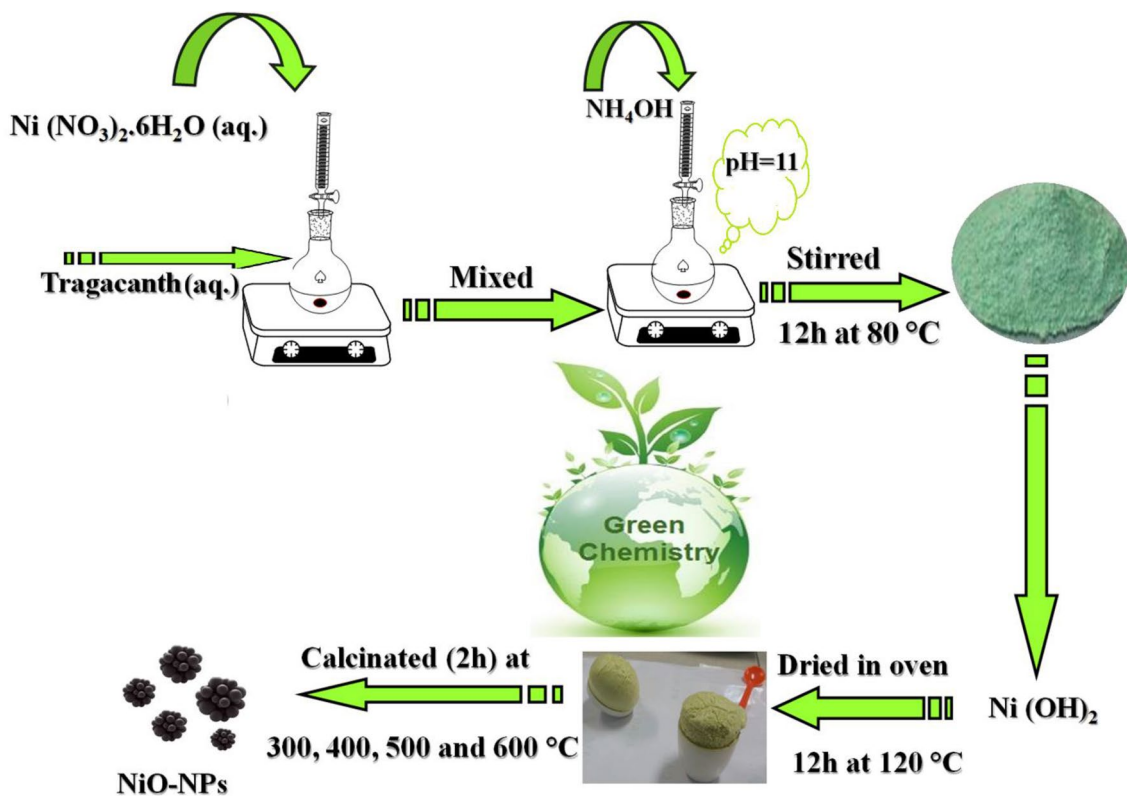


Fig. 1 Schematic plan the biosynthesis of NiO nanosheets

NiO nanosheets as well. Moreover, the optical properties of tragacanth-stabilized NiO nanosheets have been investigated through the means of UV–Vis spectroscopy (UV–Vis 2550-SHIMADZU Made in the USA). For this purpose, the synthesized powder has been initially dispersed uniformly in deionized water by ultrasonic device and then, the synthesized powder has been identified in terms of absorption spectrum at 200–800 nm.

### Investigation photocatalytic activity of tragacanth-stabilized NiO nanosheets

The photocatalytic process contains a vital functionality in the cleansing of polluted water. In this respect, NiO has been applied as the photocatalyst for the degradation of methylene blue (MB) and methyl orange (MO) dyes under UVA light irradiation [30, 31]. In the presence of UVA (11 W) light irradiation, it is quite challenging to decompose MB dye without a catalyst, as it is proved in Fig. 3a. However, the photocatalytic degradation of MB dye has been detected in the presence of NiO nanosheets by photon absorption. The schematic mechanism of photocatalytic degradation of MB and MO dyes are presented in Fig. 2.

Also, electron–hole creation is a powerful instrument to oxidize/reduce organic pollutants (MB and MO dyes) [32–34]. In this process, water molecules are adsorbed on the NiO surface and trapped in the hole, causing hydroxyl radicals with oxidation. Besides, anionic superoxide radicals are produced by oxygen molecules [35]. Also, OH and anionic superoxide radicals are degraded by organic dyes dye to  $H_2O$ ,  $CO_2$ , and  $SO_4$ .

The photocatalytic activity diagram of tragacanth-stabilized NiO nanosheets to MB dye decomposition is presented in Fig. 3b. By increasing the irradiation time, the concentration of MB color has been observed to decrease, and the obtained percentage of degradation MB has been about 60% after 300 min. The contact time has been studied

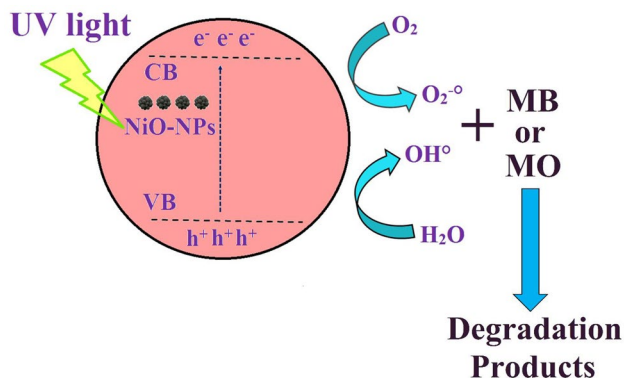


**Fig. 2** Schematic representation for degradation of MB and MO on UV light irradiation

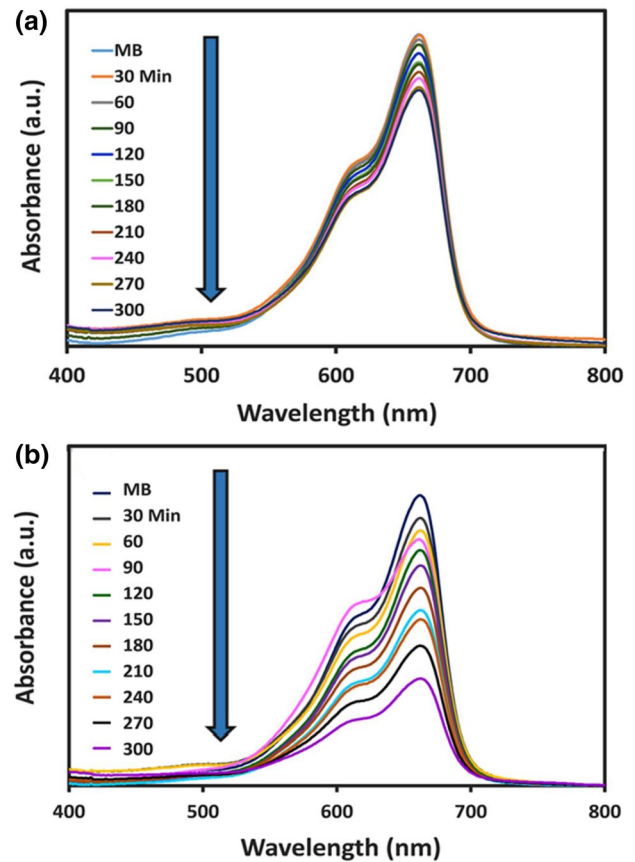


**Fig. 3** Decomposition of MB in the absence of NiO nanosheets (a) Decomposition of MB using NiO nanosheets under UVA light irradiation (b)

as a variable factor to investigate the reaction kinetics. As it has been observed through the results of kinetics experiment (Fig. 4), the photocatalytic process that contained a very high correlation coefficient ( $R$ ) has followed first-order

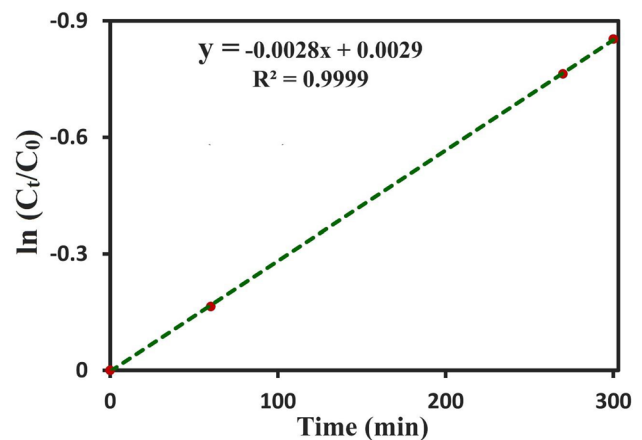


**Fig. 4** The linear plot of the pseudo-first-order kinetic model of MB degradation using NiO nanosheets

kinetics [36]. In accordance with the calculated  $k_{obs}$ , the reaction rate constant has been detected to be  $28 \cdot 10^{-3} \text{ min}^{-1}$  (Eq. 2) [37].

$$\text{Ln}\left(\frac{C_t}{C_0}\right) = K_{obs}t \tag{2}$$

where,  $C_0$  is the concentration ago of light,  $C_t$  stands as the concentration at any moment, and  $K_{obs}$  represents the observed rate constant.

Methyl orange (MO) is an anionic dye and one of the most critical pollutants in industrial wastewater, which is resistant to light degradation and had been selected for the removal and evaluation of photocatalytic activity. The evaluation of MO photocatalytic test has been performed in acidic medium (pH 3) and its maximum absorption has been observed at 464 nm. Throughout intervals of 30 min, the solution has been continuously irradiated (0, 30, 60, 90, 120, 150, 180, 210, and 240 min) under UVA light. The photocatalytic activity diagram of tragacanth-stabilized NiO nanosheets in regards to MO decomposition is presented in Fig. 5. As the irradiation time had been increased, the concentration of methyl orange color has faced a decrease, and the percentage of degradation methyl orange has been estimated to be about 84% after 210 min.

**XRD pattern**

Figure 6 illustrates the XRD pattern of tragacanth-stabilized NiO nanosheets at the temperatures of 300, 400, 500, and 600 °C while being at the  $2\theta$  range of 20–80°. NiO crystalline nanosheets have displayed peaks at (111), (200), (220), (311), and (222) planes, which had been in correspondence to the standard XRD pattern (JCPDS Card No. 47–1049)

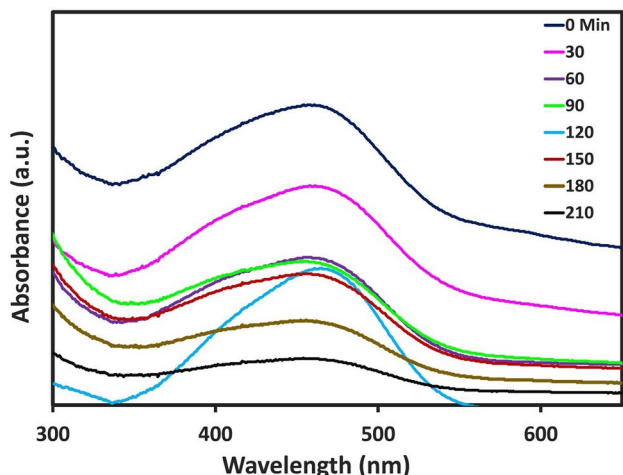


Fig. 5 Degradation of MO using NiO nanosheets under UVA light irradiation

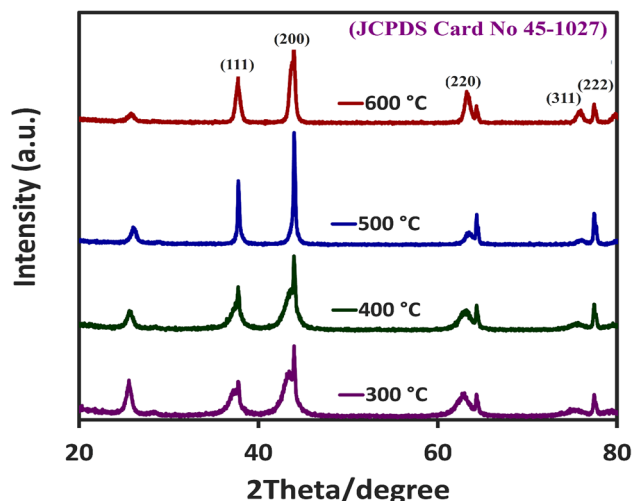


Fig. 6 The XRD pattern of NiO nanosheets at 300, 400, 500, and 600 °C

[38, 39]. All of the peaks have signified the pure synthesis of NiO nanosheets, which contained a cubic structure and space group of Fm3m [39, 40]. Phase structure analysis has shown the purification and crystallization of NiO nanosheets, in which there has not been any other peaks related to impurities that could be observed throughout the XRD pattern. Nevertheless, this does not mean that all of the synthesized samples contain only pure NiO and it is necessary to consider the presence of amorphous impurities that cannot be detected by XRD analysis. The size average of nanosheets has been obtained through the usage of Scherrer equation Eq. (3) [41]:

$$D = \frac{k\lambda}{\beta \cos\theta} \tag{3}$$

where  $\lambda$  is the wavelength (0.15406 nm),  $\theta$  would be the irradiation angle,  $k$  stands as a constant (0.9), and  $D$  is the nanosheets size (nm). According to Fig. 6 and Table 1, as the calcination temperature had been heightened, the corresponding peaks to Ni(OH)<sub>2</sub> has disappeared as well. Moreover, by increasing the calcination temperature, the width of peaks has decreased due to the extended tendency

Table 1 Comparison of particle size of as-synthesized NiO nanosheets

Temp. (°C)	2θ (deg.)	FWHM (rad.)	Diameter (nm)	Identification
300	43.97	0.0984	18	[(fcc [NiO + Ni]
400	42.84	0.3149	29	[(fcc [NiO + (Ni]
500	42.84	0.4723	20	[(fcc [NiO + (Ni]
600	42.88	0.2165	43	fcc [NiO + (Ni]

to aggregate nanosheets, while their size had become more prominent [42].

### UV–Vis analysis

In Fig. 7a, b displays the UV–Vis spectra and bandgap of synthesized NiO nanosheets at the temperatures of 300, 400, 500, and 600 °C. The optical absorption spectra have been measured by dispersing NiO nanosheets in water throughout the range of 200 – 800 nm. The obtained nanosheets have shown excitation peaks at 257, 274, 296, and 305 nm at different temperatures that had been related to the electron transfer from O (2p) Orbital to Ni(3d) Orbital ( $O_{2p} \rightarrow Ni_{3d}$ ) [43–45], which indicated the presence of NiO nanosheets that were measured at room temperature. As it is shown in Fig. 7, by heightening the temperature and reducing the average size of nanosheets, their wavelength has decreased and the bandgap energy had faced an increase. Also, the bandgap energy of NiO nanosheets has been determined by Eq. 4 [46].

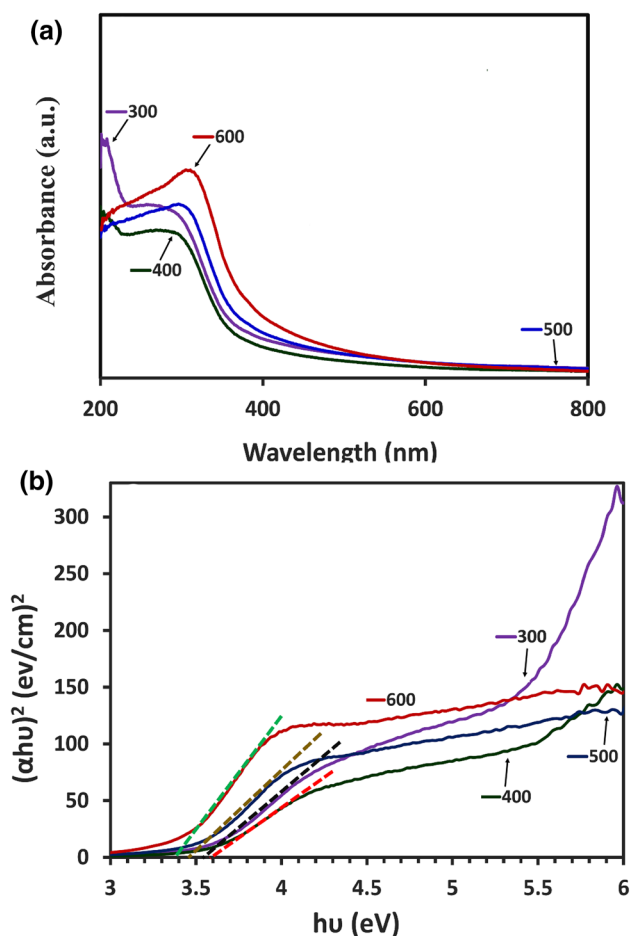


**Fig. 7** UV–Vis (a)/bandgap, (b) spectra of NiO nanosheets at 300, 400, 500, and 600 °C

$$(\alpha h\nu)^n = A(h\nu - E_g) \quad (4)$$

In this equation,  $A$  stands as a fixed number,  $\alpha$  is the absorption coefficient,  $h\nu$  would be the photon energy,  $E_g$  represents the energy of bandgap, and  $n$  is equalled to 2 for permitted direct transfers and equivalent to 1/2 for permitted indirect transfers. The  $(\alpha h\nu)^2$  curve has been plotted in the order of  $h\nu$  to determine the  $E_g$  of nanosheets and considering the linear extrapolation of graphs, the  $E_g$  has been obtained and presented in Table 2.

### FT-IR spectra

The FT-IR spectra of NiO nanosheets have been determined through the wavenumber range of 4000 to 400  $cm^{-1}$  at 300, 400, 500, and 600 °C (Fig. 8). Broad peaks that correspond to 3445  $cm^{-1}$  range have signified the presence of O–H stretch vibrations. The observation band at 1625  $cm^{-1}$  range has indicated the stretching vibration of C=O group, which is probably due to the remaining traga-canth in the composition. The existing peak at 1130  $cm^{-1}$  field has been related to the bending vibrations of water molecules [37, 47]. FT-IR has revealed signs of synthesis and stabilization that might be due to the groups that were involved in capping and reduction processes [48]. The

**Table 2** The UV–Vis spectral data and the energy bandgap of NiO nanosheets

Parameter	Temperature (°C)			
	300	400	500	600
Wavelength (nm)	257	274	296	305
Absorbance	0.956	0.815	0.958	1.147
Energy gap (eV)	3.58	3.58	3.47	3.36

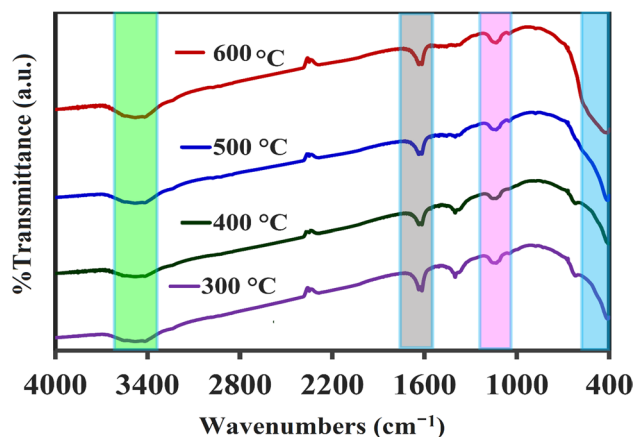


**Fig. 8** FT-IR spectra of NiO nanosheets at 300, 400, 500, and 600 °C

band that had appeared in the range of 400–450  $\text{cm}^{-1}$  has been related to the Ni–O stretching vibrations [42].

**FESEM and EDX analysis**

The FESEM /EDX images and particle size analysis (PSA) of synthesized tragacanth-stabilized NiO nanosheets at 400 °C are presented in Fig. 9a–c. FESEM analysis has been applied to examine the morphology and size of nanosheets. Figure 9a, b demonstrates the FESEM images

of synthesized tragacanth-stabilized NiO nanosheets at the scales of 200 and 500 nm, and as it is shown, their morphology is sheet-shaped or plate-like. The results that had been obtained from EDX analysis, being related to the study of constituent elements and purity of product [49], are exhibited in Fig. 9c. The indicated peaks are appropriate for nickel, oxygen, and gold. The utilized gold has been meant for preparing the sample of EDX and FESEM analysis, as well as coating nickel oxide powder on gold strips to perform the assigned analysis. The amount of

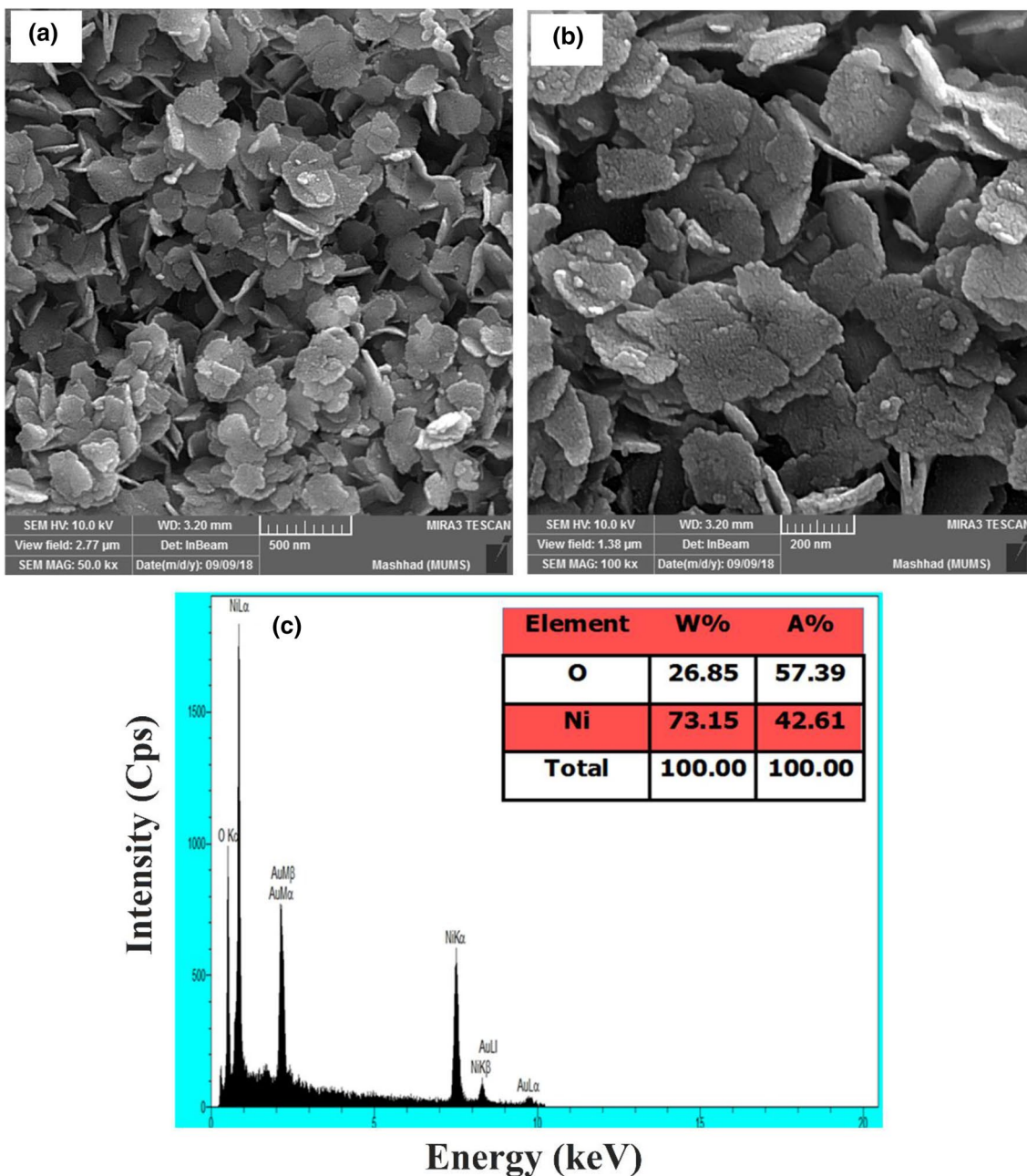
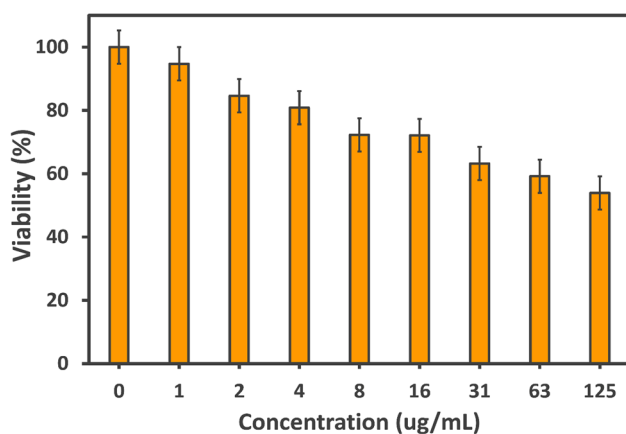


Fig. 9 The FESEM images (a, b) and EDX analysis (c) of NiO nanosheets at 400 °C

nickel in the synthesized powder has been 73.15%, while oxygen has been observed to be 26.85%, confirming that the produced nanosheets are pure without any trace of other elemental impurities.

### Evaluation of cytotoxicity effects to MTT assay

Generally, the MTT test is used to measure the toxicity of a chemical compound or any other materials on cells [50]. MTT (3-(4,5-dimethylthiazol-2-yl)-2,5-diphenyltetrazolium bromide) is a yellow tetrazolium salt that is absorbed into the mitochondria of activated metabolic cells, and due to the activity of dehydrogenase enzymes, the violet-colored formazan crystals are produced and dissolved in a suitable solvent. In this study, human Glioblastoma cancer (U87MG) cell lines have been used and cultured in a DMEM medium by 10% FBS and incubated at 37 °C in a 5% CO<sub>2</sub> atmosphere. Briefly, U87 cells have been cultivated in 96-well plates for 24 h to grow and become attached to the floor of each well. Then, the cells have been treated with various concentrations of tragacanth-stabilized NiO nanosheets for 48 h. Afterward, the environment of each well has been replaced with 200 µL of a solution that had contained 180 µL of fresh culture medium and 20 µL of MTT and incubated for 4 h. In the following, the contents of well have been exhausted and 100 µL of DMSO, which is a solvent for formazan crystals, had been appended to each well. The absorption amount of well has been determined at 540 nm through the employment of an ELISA reader [51]. The absorption ratio has displayed the amount of cell survival in each concentration, regarding the proportion of treatment group cells to control group (zero concentration), while the inhibitory concentration had been considered to be the 50% of cells that tragacanth-stabilized NiO nanosheets had destroyed



**Fig. 10** Cell viability of NiO nanosheets on Glioblastoma cancer (U87MG) cell lines by the MTT assay

(IC<sub>50</sub> = 125 µg/mL). Also, cell viability at a concentration of 31 µg/mL has been perceived to be about 63%. [52]. The results of MTT assay have shown that NiO nanosheets had the highest cytotoxicity on U87MG cell lines at a concentration of 125 µg/mL. The cytotoxicity of NiO nanosheets on U87MG cancer cells is dependent on dose and time, while these factors can be used for therapeutic purposes in future by performing further studies and targeting these nanosheets as a drug carrier. The vitro cytotoxicity studies of tragacanth-stabilized NiO nanosheets have been demonstrated in Fig. 10.

### Conclusion

The control morphology and size of tragacanth-stabilized NiO nanosheets contain an essential role in enhancing the performance of nickel oxide. It has been concluded from the results that the synthesized tragacanth-stabilized NiO nanosheets have high efficiency in regards to MO and MB dyes degradation and can be recycled as an active photocatalyst for dyes degradation of colored wastewater. Based on the outcomes, the adsorbent capacity has been estimated to be about 82% for anionic dyes (MO) and 60% for cationic dyes (MB), while the highest color degradation has been observed in acidic medium (pH 3). The findings of FTIR analyses have pointed out the formation of NiO nanosheets, and the XRD analysis has proved the purity of synthesized tragacanth-stabilized NiO nanosheets. According to the outcomes of UV–Vis spectra, a reduction in the size of nanosheets can cause an increase in the existing bandgap energy ( $E_g$ ) between the valence band and conduction band. The results of FESEM images have shown that the dimensions of NiO nanosheets are in nanoscale and contain sheet morphology. As it has been suggested by the results of MTT assay, these particular nanosheets have caused the highest cytotoxicity on U87MG cell lines at a concentration of 125 µg/mL.

**Acknowledgements** The technical support for this work has been provided by Payame Noor University of Mashhad and Mashhad University of Medical Sciences based on the Ph.D. thesis of Ms. Z. Sabouri.

### Compliance with ethical standards

**Conflict of interest** The authors declare that they have no conflict of interest.

### References

1. Sheikhshoae M, Sheikhshoae I, Karimi-Maleh H, Ranjbar M (2017) Synthesis and characterization of NiO nanoparticles by thermolysis of a Ni (II) Hydrazonic Schiff base complex. In: The first conference on the development of science and chemical industry, 1–2 Feb 2017



2. Gleiter H (2000) Nanostructured materials: basic concepts and microstructure. *Acta Mater* 48:1–29
3. Kalpana V, Devi Rajeswari V (2018) A review on green synthesis, biomedical applications, and toxicity studies of ZnO NPs. *Bioinorg Chem Appl* 2018:3569758. <https://doi.org/10.1155/2018/3569758>
4. Wang J, Liang J, Wu J, Xuan C, Wu Z, Guo X, Lai C, Zhu Y, Wang D (2018) Coordination effect of network NiO nanosheet and a carbon layer on the cathode side in constructing a high-performance lithium-sulfur battery. *J Mater Chem A* 6:6503–6509
5. Khan MM, Adil SF, Al-Mayouf A (2015) Metal oxides as photocatalysts. *J Saudi Chem Soc* 19:462–464
6. Shin JW, Choi SH, Kim DE, Kim HS, Lee J-H, Lee IS, Lee EY (2011) Heterologous expression of an alginate lyase from *Streptomyces* sp. ALG-5 in *Escherichia coli* and its use for the preparation of the magnetic nanoparticle-immobilized enzymes. *Bioprocess Biosyst Eng* 34:113–119
7. Yang J, Hou B, Wang J, Tian B, Bi J, Wang N, Li X, Huang X (2019) Nanomaterials for the removal of heavy metals from wastewater. *Nanomaterials* 9:424
8. Zalapa-Garibay MA, Torres-Torres D, Arizmendi-Morquecho AM, Reyes-López SY (2019) Effect of NiO and MoO<sub>3</sub> addition on the crystallinity and mechanical properties of  $\alpha$ -cordierite and  $\beta$ -cordierite in the MgO–Al<sub>2</sub>O<sub>3</sub>–SiO<sub>2</sub> system. *Results Phys* 13:102227
9. Alimoradzadeh R, Assadi A, Nasser S, Mehrasbi MR (2012) Photocatalytic degradation of 4-chlorophenol by UV/H<sub>2</sub>O<sub>2</sub>/NiO process in aqueous solution. *Iran J Environ Health Sci Eng* 9:12
10. Khan MM, Ansari SA, Pradhan D, Ansari MO, Han DH, Lee J, Cho MH (2014) Band gap engineered TiO<sub>2</sub> nanoparticles for visible light-induced photoelectrochemical and photocatalytic studies. *J Mater Chem A* 2:637–644
11. Sun B, Zhou G, Gao T, Zhang H, Yu H (2016) NiO nanosheet/TiO<sub>2</sub> nanorod-constructed p–n heterostructures for improved photocatalytic activity. *Appl Surf Sci* 364:322–331
12. Diallo A, Kaviyarasu K, Ndiaye S, Mothudi B, Ishaq A, Rajendran V, Maaza M (2018) Structural, optical and photocatalytic applications of biosynthesized NiO nanocrystals. *Green Chem Lett Rev* 11:166–175
13. Nourbakhsh F, Mohsennia M, Pazouki M (2017) Nickel oxide/carbon nanotube/polyaniline nanocomposite as bifunctional anode catalyst for high-performance *Shewanella*-based dual-chamber microbial fuel cell. *Bioprocess Biosyst Eng* 40:1669–1677
14. Rasalingam S, Peng R, Koodali RT (2014) Removal of hazardous pollutants from wastewaters: applications of TiO<sub>2</sub>-SiO<sub>2</sub> mixed oxide materials. *J Nanomater* 2014:10
15. Johar MA, Afzal RA, Alazba AA, Manzoor U (2015) Photocatalysis and bandgap engineering using ZnO nanocomposites. *Adv Mater Sci Eng* 2015:934587. <https://doi.org/10.1155/2015/934587>
16. Dong Q, Yin S, Guo C, Wu X, Kumada N, Takei T, Miura A, Yonesaki Y, Sato T (2014) Single-crystalline porous NiO nanosheets prepared from  $\beta$ -Ni(OH)<sub>2</sub> nanosheets: magnetic property and photocatalytic activity. *Appl Catal B* 147:741–747
17. Darroudi M, Sabouri Z, Kazemi Oskuee R, Khorsand Zak A, Kargar H, Hamid MHNA (2013) Sol–gel synthesis, characterization, and neurotoxicity effect of zinc oxide nanoparticles using gum tragacanth. *Ceram Int* 39:9195–9199
18. Balaghi S, Mohammadifar MA, Zargaraan A, Gavlighi HA, Mohammadi M (2011) Compositional analysis and rheological characterization of gum tragacanth exudates from six species of Iranian *Astragalus*. *Food Hydrocoll* 25:1775–1784
19. Zare EN, Makvandi P, Borzacchiello A, Tay FR, Padil VVT (2019) Antimicrobial gum bio-based nanocomposites and their industrial and biomedical applications. *Chem Commun* 55:14871–14885
20. Darroudi M, Sabouri Z, Kazemi Oskuee R, Kargar H, Hosseini HA (2014) Neuronal toxicity of biopolymer-template synthesized ZnO nanoparticles. *Nanomed J* 1:88–93
21. Thiruvengadam M, Chung I-M, Gomathi T, Ansari MA, Khanna VG, Babu V, Rajakumar G (2019) Synthesis, characterization and pharmacological potential of green synthesized copper nanoparticles. *Bioprocess Biosyst Eng* 42:1769–1777
22. Syafiuddin A, Hadibarata T, Salim MR, Kueh ABH, Sari AA (2017) A purely green synthesis of silver nanoparticles using *Carica papaya*, *Manihot esculenta*, and *Morinda citrifolia*: synthesis and antibacterial evaluations. *Bioprocess Biosyst Eng* 40:1349–1361
23. Khan ME, Khan MM, Min B-K, Cho MH (2018) Microbial fuel cell assisted band gap narrowed TiO<sub>2</sub> for visible light-induced photocatalytic activities and power generation. *Sci Rep* 8:1723
24. Baghayeri M, Mahdavi B, Hosseini-Mohsen Abadi Z, Farhadi S (2018) Green synthesis of silver nanoparticles using water extract of *Salvia leuifolia*: antibacterial studies and applications as catalysts in the electrochemical detection of nitrite. *Appl Organomet Chem* 32:e4057
25. Akbari A, Khammar M, Taherzadeh D, Rajabian A, Zak AK, Darroudi M (2017) Zinc-doped cerium oxide nanoparticles: Sol–gel synthesis, characterization, and investigation of their in vitro cytotoxicity effects. *J Mol Struct* 1149:771–776
26. Zhu Y, Cao C, Tao S, Chu W, Wu Z, Li Y (2014) Ultrathin nickel hydroxide and oxide nanosheets: synthesis, characterizations, and excellent supercapacitor performances. *Sci Rep* 4:5787
27. Wu Z, Jiang L, Zhu Y, Xu C, Ye Y, Wang X (2012) Synthesis of mesoporous NiO nanosheet and its application on mercury (II) sensor. *J Solid State Electrochem* 16:3171–3177
28. She S, Bian S, Huo R, Chen K, Huang Z, Zhang J, Hao J, Wei Y (2016) Degradable organically-derivatized polyoxometalate with enhanced activity against glioblastoma cell line. *Sci Rep* 6:33529
29. Gao H, Yang Z, Cao S, Xiong Y, Zhang S, Pang Z, Jiang X (2014) Tumor cells and neovasculature dual targeting delivery for glioblastoma treatment. *Biomaterials* 35:2374–2382
30. Senobari S, Nezamzadeh-Ejhi A (2018) A p–n junction NiO–CdS nanoparticles with enhanced photocatalytic activity: a response surface methodology study. *J Mol Liq* 257:173–183
31. Ramesh M, Rao MPC, Anandan S, Nagaraja H (2018) Adsorption and photocatalytic properties of NiO nanoparticles synthesized via a thermal decomposition process. *J Mater Res* 33:601–610
32. Balamurugan S, Balu AR, Narasimman V, Selvan G, Usharani K, Srividya J, Suganya M, Manjula N, Rajashree C, Nagarethinam VS (2019) Multimetal oxide CdO–Al<sub>2</sub>O<sub>3</sub>–NiO nanocomposite-synthesis, photocatalytic and magnetic properties. *Mater Res Exp* 6(1):015022
33. Mardiroosi A, Mahjoub AR, Fakhri H (2017) Efficient visible-light photocatalytic activity based on magnetic graphene oxide decorated ZnO/NiO. *J Mater Sci Mater Electron* 28:11722–11732
34. Najafian H, Manteghi F, Beshkar F, Salavati-Niasari M (2019) Enhanced photocatalytic activity of a novel NiO/Bi<sub>2</sub>O<sub>3</sub>/Bi<sub>3</sub>ClO<sub>4</sub> nanocomposite for the degradation of azo dye pollutants under visible light irradiation. *Sep Purif Technol* 209:6–17
35. Ezhilarasi AA, Vijaya JJ, Kaviyarasu K, Kennedy LJ, Ramalingam RJ, Al-Lohedan HA (2018) Green synthesis of NiO nanoparticles using *Aegle marmelos* leaf extract for the evaluation of in-vitro cytotoxicity, antibacterial and photocatalytic properties. *J Photochem Photobiol B Biol* 180:39–50
36. Farouq R (2018) Investigation of the kinetics and optimization of photocatalytic degradation of methylene blue. *J Chin Chem Soc* 65:1333–1339
37. Sabouri Z, Akbari A, Hosseini HA, Hashemzadeh A, Darroudi M (2019) Bio-based synthesized NiO nanoparticles and evaluation of their cellular toxicity and wastewater treatment effects. *J Mol Struct*

38. Ahamed M, Ali D, Alhadlaq HA, Akhtar MJ (2013) Nickel oxide nanoparticles exert cytotoxicity via oxidative stress and induce an apoptotic response in human liver cells (HepG2). *Chemosphere* 93:2514–2522
39. Xiao H, Yao S, Liu H, Qu F, Zhang X, Wu X (2016) NiO nanosheet assembles for supercapacitor electrode materials. *Prog Nat Sci Mater Int* 26:271–275
40. Bose P, Ghosh S, Basak S, Naskar MK (2016) A facile synthesis of mesoporous NiO nanosheets and their application in CO oxidation. *J Asian Ceram Soc* 4:1–5
41. Derakhshi M, Jamali T, Elyasi M, Bijad M, Sadeghi R, Kamali A, Niazazari K, Shahmiri MR, Bahari A, Mokhtari S (2013) Synthesis and characterization of NiO nanoparticle as a high sensitive voltammetric sensor for vitamin C determination in food samples. *Int J Electrochem Sci* 8:8252–8263
42. Sabouri Z, Akbari A, Hosseini HA, Hashemzadeh A, Darroudi M (2019) Eco-friendly biosynthesis of nickel oxide nanoparticles mediated by okra plant extract and investigation of their photocatalytic, magnetic, cytotoxicity, and antibacterial properties. *J Clust Sci*
43. Shukla A, Rueff J-P, Badro J, Vanko G, Mattila A, de Groot FF, Sette F (2003) Charge transfer at very high pressure in NiO. *Phys Rev B* 67:081101
44. Karunamoorthy S, Velluchamy M (2018) Design and synthesis of bandgap tailored porous Ag/NiO nanocomposite: a sufficient visible light active photocatalyst for degradation of organic pollutants. *J Mater Sci Mater Electron* 29:20367–20382
45. Liu H, Guo Y, Wang N, Liu B, Zhang Y, Liu H, Chen R (2019) Controllable synthesis and photocatalytic activity of ultrathin hematite nanosheets. *J Alloy Compd* 771:343–349
46. Sabouri Z, Fereydouni N, Akbari A, Hosseini HA, Hashemzadeh A, Amiri MS, Oskuee RK, Darroudi M (2019) Plant-based synthesis of NiO nanoparticles using salvia macrosiphon Boiss extract and examination of their water treatment. *Rare Met.* <https://doi.org/10.1007/s12598-019-01333-z>
47. Khandannasab N, Sabouri Z, Ghazal S, Darroudi M (2019) Green-based synthesis of mixed-phase silver nanoparticles as an effective photocatalyst and investigation of their antibacterial properties. *J Mol Struct* 127411
48. Amoresi RA, Felix AA, Botero ER, Domingues NL, Falcão EA, Zaghete MA, Rinaldi AW (2015) Crystallinity, morphology and high dielectric permittivity of NiO nanosheets filling poly (vinylidene fluoride). *Ceram Int* 41:14733–14739
49. Sabouri Z, Akbari A, Hosseini HA, Darroudi M (2018) Facile green synthesis of NiO nanoparticles and investigation of dye degradation and cytotoxicity effects. *J Mol Struct* 1173:931–936
50. Darroudi M, Sabouri Z, Kazemi Oskuee R, Khorsand Zak A, Kargar H, Abd Hamid MHN (2014) Green chemistry approach for the synthesis of ZnO nanopowders and their cytotoxic effects. *Ceram Int* 40:4827–4831
51. Kora AJ, Sashidhar R (2018) Biogenic silver nanoparticles synthesized with rhamnogalacturonan gum: antibacterial activity, cytotoxicity, and its mode of action. *Arab J Chem* 11:313–323
52. van Meerloo J, Kaspers GJ, Cloos J (2011) Cell sensitivity assays: the MTT assay. *Cancer cell culture*. Springer, Berlin

**Publisher's Note** Springer Nature remains neutral with regard to jurisdictional claims in published maps and institutional affiliations.